Theory of liquid-mediated strain release in two-dimensional materials

H. Batiz, Ji Guo, Geun Ho Ahn, Hyungjin Kim, Ali Javey, J. W. Ager, III, and D. C. Chrzan

Theory of liquid-mediated strain release in two-dimensional materials

H. Batiz,[1,2] Ji Guo,[1,2] Geun Ho Ahn,[3,2] Hyungjin Kim,[3,2] Ali Javey,[3,2] J. W. Ager III,[1,2] and D. C. Chrzan[2,1,*]

[1]*Department of Materials Science and Engineering,*
University of California,Berkeley, CA 94720, USA
[2]*Materials Sciences Division, Lawrence Berkeley National Laboratory, Berkeley, CA 94720, USA*
[3]*Department of Electrical Engineering and Computer Sciences,*
University of California,Berkeley, CA 94720, USA

Strain engineering in transition metal dichalcogenides is an important means to manipulate these materials' electronic and optical properties. Recently, it has been shown that WSe_2 monolayers grown on fused silica substrates using chemical vapour deposition can retain residual strain due to thermal expansion mismatch. Moreover, it was demonstrated that this strain can be released using a solvent-evaporation mediated decoupling method. A continuum theory to explain these observations is introduced and its predictions analyzed. The theory is used to establish that it is plausible that bonds much weaker than typical covalent bonds are sufficient to stabilize strains in the range of those experimentally observed. It is shown that the presence of the solvent modifies the equilibrium in-plane displacement of the film, while its lifting is negligible. Under the proper conditions, this displacement leads to an increase in the decoupling force, thereby initiating the strain relief process. The theory clarifies the role of the liquid surface tension in the relaxation process, and identifies the relationships between droplet wetting behavior and initial strain state that will lead to solute-evaporation mediated decoupling.

I. INTRODUCTION

Two-dimensional transition metal dichalcogenides (2D TMDCs) have been researched intensely due to their fascinating properties[1,2]. Moreover, it has been proven that their optical and electronic properties can be strain engineered[3–5]. Accordingly, the need for a method by which the strain in 2D materials can be controlled has become more pressing.

Recently, it was shown that WSe$_2$ monolayers synthesized using chemical vapour deposition are able to retain some of the strain arising from the mismatch in thermal coefficients of expansion (TCE) between the film and the substrate, while still retaining their intrinsic optoelectronic properties[6]. This observation is intriguing, as the strain was retained for films grown on amorphous substrates. While strain stabilization arising from crystalline epitaxial growth is well documented, one might expect that remnant thermal mismatch strain mediated by van der Waals bonding to a substrate would be relaxed during cooling from the growth temperature, as the bonding between the film and substrate is relatively weaker.

Since the strain is mediated by the bonding between the film and substrate, the strain should be relieved if the film decouples from the substrate. A method to release the TCE mismatch induced strain in WSe$_2$ mono- and bilayers was recently presented[7]. This solvent-evaporation mediated decoupling (SEMD) process consists in letting a droplet of acetone *evaporate* on top of a strained WSe$_2$ film grown on amorphous silica. The decoupling refers to the supposition that the droplet evaporation enables the film to slip upon the substrate so as to reduce its internal strain while still remaining bonded to the substrate. The strain in the 2D TMDC is released as the film-liquid-vapor triple contact line sweeps over the film. The stress in the films relaxes from the edges inward, as is shown through time-dependent photoluminescence experiments[7]. In contrast, no strain relaxation is observed when the film is completely submerged in acetone.

The effectiveness of the SEMD process raises (at least) three interesting questions. First, are the bonds formed during van der Waals epitaxy sufficiently strong to sustain the strain, or must there be some number of covalent bonds between the film and the substrate? Second, what is the nature of the perturbation to the film induced by the presence of the acetone that allows for decoupling of the film and the substrate? Third, what are the conditions under which SEMD will be operative?

In the following, these questions are addressed by analyzing a continuum model that considers the balance of surface tension and elastic forces as the liquid evaporates from the film. Section II introduces the continuum model, and establishes that bonds in the strength range of van der Waals bond are capable of maintaining the strain within the film. The forces that arise when the droplet is placed on the film are also presented, and it is argued that liquid/vapor/film interface results in an additional *in-plane* force on the decoupling front. Section III presents an analysis of the relationship between the in-plane force and the wetting behavior of the liquid droplet. Specifically the wetting behaviors and initial strain states for which SEMD is possible are identified. Section IV presents the conclusions.

II. MODEL

The geometry of a simple continuum model used to explore SEMD is displayed in Fig. 1. The WSe$_2$ sample is assumed to adhere to the substrate under an initial tensile radial strain of ε_o imposed by TCE mismatch between the substrate and the film. For simplicity, the film is assumed to be circular, so that an axisymmetric model can be applied. The elastic contributions to the film energy are modeled within linear continuum elasticity theory and the contributions of the droplet to the energy of the system are modeled using a continuum theory as well. A droplet of solvent is placed on the center of the film (initially covering the entire film). The droplet is assumed to be a spherical cap (gravity is neglected). In the unstrained WSe$_2$ monolayer material coordinates (Fig. 1b), the radius of the circle defined by the intersection of the droplet and WSe$_2$ film is defined to be r_0, with r_0 decreasing to zero as the droplet evaporates. As noted above, the WSe$_2$ monolayer is expected to decouple from the edges inward[7], and this decoupled region is demarcated by the dashed line at radius Δ in Fig. 1b. Points in the WSe$_2$ monolayer with $r > \Delta$, *i.e.* those points in the decoupled region, are assumed to remain bound to the substrate, but able to slide without friction; the model neglects re-adherence of the film after slipping. The evaporation rate of the acetone is assumed to be slow in comparison to the rate at which the film assumes its elastic equilibrium, so that an equilibrium static calculation suffices.

A. Magnitude of Atomic Forces Mediating Film Adhesion to the Substrate

The model is first applied to develop an understanding of the forces preventing the TCE mismatch strain from relaxing due to thermal fluctuations or other effects.
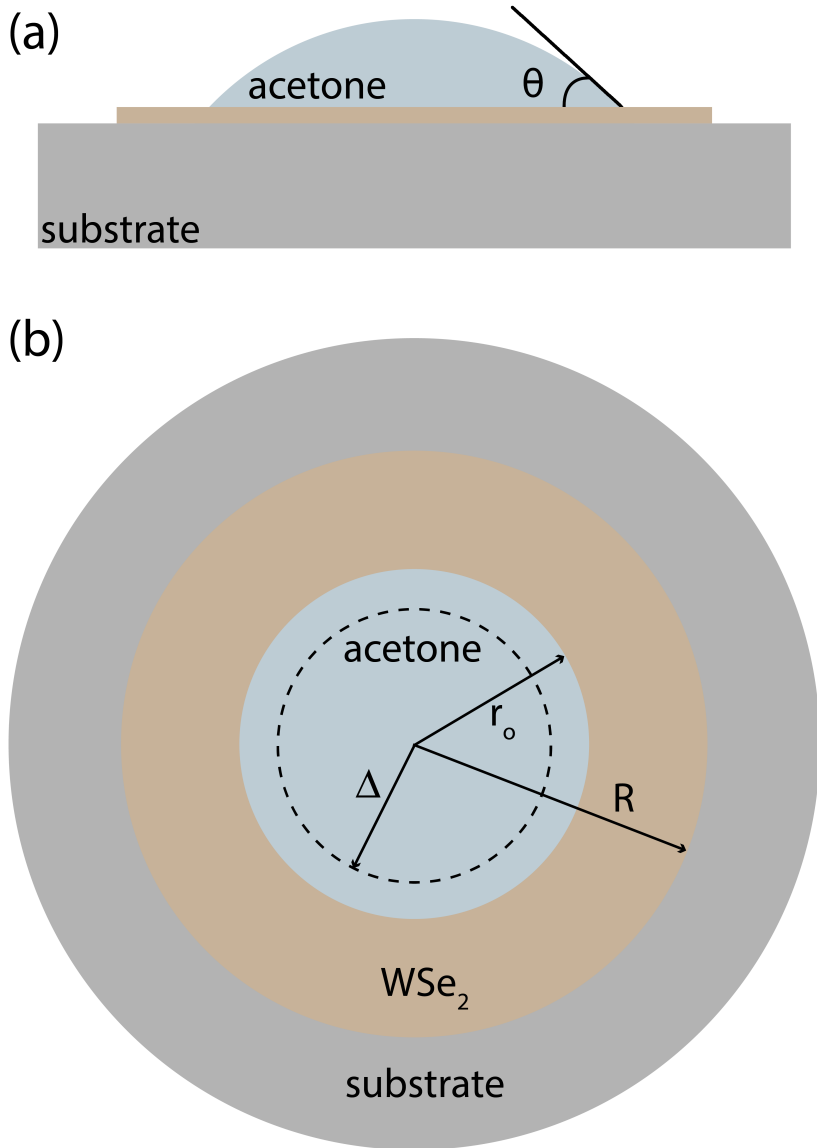
FIG. 1. A schematic of the continuum model: (a) side view and (b) top-down view. The WSe$_2$ sample is assumed to be circular in shape with unstrained radius R, and rigidly attached to the substrate within the radius Δ, again defined in the unstrained material coordinate system. The material within this radius is assumed to be under the fixed biaxial strain ε_o (that arises from the synthesis process). The radius of the contact patch between the acetone and the film is taken to be r_0, also in the unstrained material coordinate system. The contact angle in Eqn. (8) is shown.

Consider the film-substrate system without the droplet. Specifically, consider the configuration in which the film is decoupled and completely free to slide beyond a radius of Δ, and is also biaxially strained by an amount ε_o for $r < \Delta$ (Fig. 1b). One can use continuum linear elasticity theory[8] to estimate the magnitudes of the forces that the atoms near Δ must exert in order to keep the film stable.

The system is axially symmetric with a deformation map given by $r \rightarrow r + u(r)$. Within continuum linear elasticity theory (see Appendix C for details), one can show that the elastic energy in the film is given by:

$$E_{elastic}\left(\Delta\right) = 2\pi\Delta^2(\lambda+\mu)\varepsilon_o^2 + \frac{2\pi\Delta^2\mu(\lambda+\mu)\varepsilon_o^2(R-\Delta)(\Delta+R)}{\Delta^2\mu + R^2(\lambda+\mu)}, \tag{1}$$

where λ and μ are the Lamé constant and shear modulus[8] of the WSe$_2$ film, respectively. From this same analysis,

one finds that the radial displacements of the film are given by:

$$u\left(r\right) = \begin{cases} \varepsilon_o r & r < \Delta \\ \frac{\Delta^2 \varepsilon_o \left(\mu r^2 + R^2(\lambda+\mu)\right)}{r(\Delta^2 \mu + R^2(\lambda+\mu))} & r \geq \Delta \end{cases}. \tag{2}$$

The generalized force leading to decoupling of the monolayer can be computed from the elastic energy. One finds:

$$F_\Delta = -\frac{\partial E_{elastic}}{\partial \Delta} = -\frac{4\pi\Delta R^4(\lambda+\mu)^2(\lambda+2\mu)\varepsilon_o^2}{\left(\Delta^2\mu + R^2(\lambda+\mu)\right)^2}, \tag{3}$$

where the negative sign indicates that the force is acting to decrease Δ, as expected. F_Δ is plotted as a function of Δ for the parameters shown in Table I, a monolayer of radius $R = 8\,\mu m$, and initial strain of $\varepsilon_o = 0.7\%$ in Fig. 2(a), for reference. The sample size and strain were chosen to be comparable to those studied experimentally[7], though the experimental samples are triangular. Unless otherwise noted, these parameters will be used throughout the study.

To make a quantitative estimate of the bond forces necessary to retain the strain, consider the following model. Suppose that the atoms within the $\Delta - \delta < r < \Delta$ annulus slip so as to relieve the strain within the annulus. Also assume that the atoms with positions such that $r > \Delta$ remain decoupled from the substrate, so that they can slide freely on the substrate. One can estimate the average bond force on the atoms in the considered annulus by equating the reduction in elastic energy to the work those bond forces would need to do to restrain the film to its pre-slipped configuration.

The change in elastic energy upon decoupling an annulus of thickness δ starting from a strained region of radius Δ, defined to be $\Delta E_{elastic}\left(\Delta, \delta\right)$ can be approximated by

$$\Delta E_{elastic}\left(\Delta, \delta\right) \approx F_\Delta \delta. \tag{4}$$

In this sense, F_Δ sets the scale for the atomic forces, and can be used to assess the changes in these atomic forces with changing parameters. However, one can make a more accurate calculation by computing the finite difference in energy directly using Eqn. (1), so going forward, we define $\Delta E_{elastic}\left(\Delta, \delta\right) = E_{elastic}\left(\Delta - \delta\right) - E_{elastic}\left(\Delta\right)$.

The average displacement of the atoms in the $\Delta - \delta < r < \Delta$ annulus due to the motion of the decoupling front is defined to be $\bar{u}\left(\Delta, \delta\right)$. Defining the displacement of the atoms within the annulus upon motion of the pinned region boundary by δ to be $\Delta u\left(r, \delta\right)$:

$$\Delta u\left(r, \delta\right) = \frac{\varepsilon_o(\Delta - \delta)^2 \left(\mu r^2 + R^2(\lambda+\mu)\right)}{r\left(\mu(\Delta - \delta)^2 + R^2(\lambda+\mu)\right)} - \varepsilon_o r, \tag{5}$$

one finds:

$$\begin{aligned} \bar{u}_r\left(\Delta, \delta\right) &= \frac{\int_{\Delta-\delta}^{\Delta} 2\pi r \Delta u\left(r, \delta\right) dr}{\pi\left(\Delta^2 - (\Delta - \delta)^2\right)} \\ &= -\frac{2\delta R^2(2\delta - 3\Delta)(\lambda+\mu)\varepsilon_o}{3(\delta - 2\Delta)\left(\mu(\delta - \Delta)^2 + R^2(\lambda+\mu)\right)}. \end{aligned} \tag{6}$$

Using this observation, the magnitude of the average force on the atoms in the region of interest, defined to be $\bar{f}\left(\Delta, \delta\right)$, is approximated by the change in elastic energy computed using Eqn. (1) divided by the product of the number of atoms in the strip contacting the substrate and their average displacement:

$$\begin{aligned} \bar{f}\left(\Delta, \delta\right) &= \frac{\Delta E_{elastic}\left(\Delta, \delta\right) A_c}{\bar{u}_r\left(\Delta, \delta\right)\pi\left(\Delta^2 - (\Delta - \delta)^2\right)} \\ &= \frac{3R^2 A_c(\delta - 2\Delta)(\lambda+\mu)(\lambda+2\mu)\varepsilon_o}{\delta(2\delta - 3\Delta)\left(\Delta^2\mu + R^2(\lambda+\mu)\right)}, \end{aligned} \tag{7}$$

with A_c the area of the unit cell for the monolayer. $\bar{f}(\Delta, \delta)$ is plotted as a function of Δ for various values of δ in Fig. 2(b).

Care should be used in applying Eqn. (7). Examination of this expression shows that as $\delta \rightarrow 0$, the characteristic bond force diverges $\sim \delta^{-1}$. This implies that the average bond force must be infinite to keep the film coupled to the substrate. The difficulty, of course, is that the film is not an elastic continuum, and decreasing the radius of a coupled region by amounts less than the lattice parameter makes little sense. So applying the model for $\delta \sim$ lattice parameter is not likely to yield reasonable results. Moreover, the film may not relax smoothly on the scale of the lattice parameter,

but, as discussed below, it is likely to have domains of relaxation that in turn trigger other domains to relax, etc. However, a more detailed analysis requires an atomic scale model, which is beyond the scope of this work.

Importantly, for larger values of δ, the model predicts that forces of the order of $0.01\,\text{eV}/\text{Å}$ are sufficient to retain the strain for reasonable values of δ. The strength of covalent bonds is of the order of $1\,\text{eV}/\text{Å}$[9], so the bond strength necessary to sustain the strain is approximately two orders of magnitude weaker than that expected from covalent bonds. Indeed, atomic scale simulations for a strained MoS_2 monolayer system predict that, in order to maintain a tensile strain of $\sim 1\%$, forces with an order of magnitude of $0.01\,\text{eV}\,\text{Å}^{-1}$ per atom are needed[10]. The theory predicts that the average force per atom within a strip $50\,\text{Å}$ wide necessary to sustain the observed strain is of the order of $0.01\,\text{eV}\,\text{Å}^{-1}$. It is reasonable to expect that the slipping of the decoupling front will involve the correlated motion of atoms over a strip this wide[11]. It is also likely that the decoupled portion of the film will, perhaps weakly, re-adhere to the substrate, further stabilizing the strain within the film. The model, which neglects this re-adhering, will overestimate the force required for stabilization. Thus it appears that a relatively thin strip of atoms weakly bonded to the surface is able to maintain the tensile strain in the film, such that it is not necessary to invoke the presence of covalent bonds between the substrate and the film. The analysis, however, does not rule out the possibility that a small number of covalent bonds might be present.

TABLE I. Numerical values of the material properties and the methods by which they were obtained. DFPT stands for Density Functional Perturbation Theory, and γ_{sl} was computed using Eqn. (8) with $\theta = 22°$. Values are in MeV µm^{-2} units.

λ^{12}	μ^{12}	γ_{sv}[13]	γ_{lv}[14]	γ_{sl}
144	303	0.24	0.16	0.10
DFPT	Contact angle measurement	Capillary rise	Young's equation

B.   Forces on Atoms with Droplet Present

Empirically, it is known that the passage of the contact triple point across the surface of the film leads to decoupling and release of the stress. Evidently, the contact triple point increases the forces tending to decouple the film. The model in Fig. 1 reveals the origins of this increase in force.

In general, when considering static friction, one assumes that the frictional force is related to the normal force. One possible explanation for the decoupling of the film by the evaporating liquid droplet is that the droplet lifts the film, and reduces the friction force[7]. A detailed analysis of this possibility is presented in Appendix A where it is shown that the film is expected to lift approximately $0.01\,\text{Å}$, an amount that is surely negligible. Given this observation, then, the origins of the decoupling must be present in a model for which the lifting of the film is negligible. One such model is presented here.

The starting point for this model of SEMD is the exploration of the deformation of a solid in the presence of a droplet. If a droplet sits on an undeformable substrate, the contact angle obeys Young's equation[15]:

$$\gamma_{lv}\cos(\theta) + \gamma_{sl} - \gamma_{sv} = 0, \tag{8}$$

where θ is the contact angle between the substrate and the liquid (Fig. 1); the subscripts l, v, s stand for liquid, vapor and solid, respectively; and γ_{ij} is the specific interfacial free energy of the ij interface. It is well known, however, that if the substrate is deformable, Eqn. (8) is no longer valid[16–24]. While there are several models describing this system[22,25–27], the film under consideration is bound to a substrate that resists the vertical deflection, as noted above.

Therefore, we suppose that a spherical cap droplet is supported by a material that is only allowed to have in-plane deformation. Physically, this corresponds to a thin film supported on a rigid substrate, with the interaction between the film and substrate strong enough to prevent out-of-plane deformations. Considering the droplet to be centered on the film (see Fig. 1), the problem remains axisymmetric, and the deformation map can also be written as $r \rightarrow r + u(r)$. The distance from the center of the droplet to the triple contact line is defined to be $r_0 + u_0$, with $u_0 = u(r_0)$. As in the previous section, it is assumed that $u(r) = \varepsilon_o r$ if $r \leq \Delta$.

First, consider the case in which the film is submerged in liquid, i.e. $r_0 > R$. In this instance, the elastic energy of the film changes as Δ is decreased from $\Delta = R$, but the interfacial energies remain constant (in the approximation that any film strain dependence to the liquid/film interfacial free energy can be neglected); then, the system reduces to that presented in sec. II A. Similarly, if $r_0 \leq \Delta$, the deformation of the film will not have any effect on the interfacial energy of the system, as the film-liquid-vapour triple contact line sits is on the undeformable region; in this case, the forces in the system are also reduced to those computed in sec. II A. Thus for the droplet to influence the decoupling process, the edge of the droplet must fall in the film's deformable region, i.e. $\Delta < r_0 < R$, and this will be assumed in what follows.
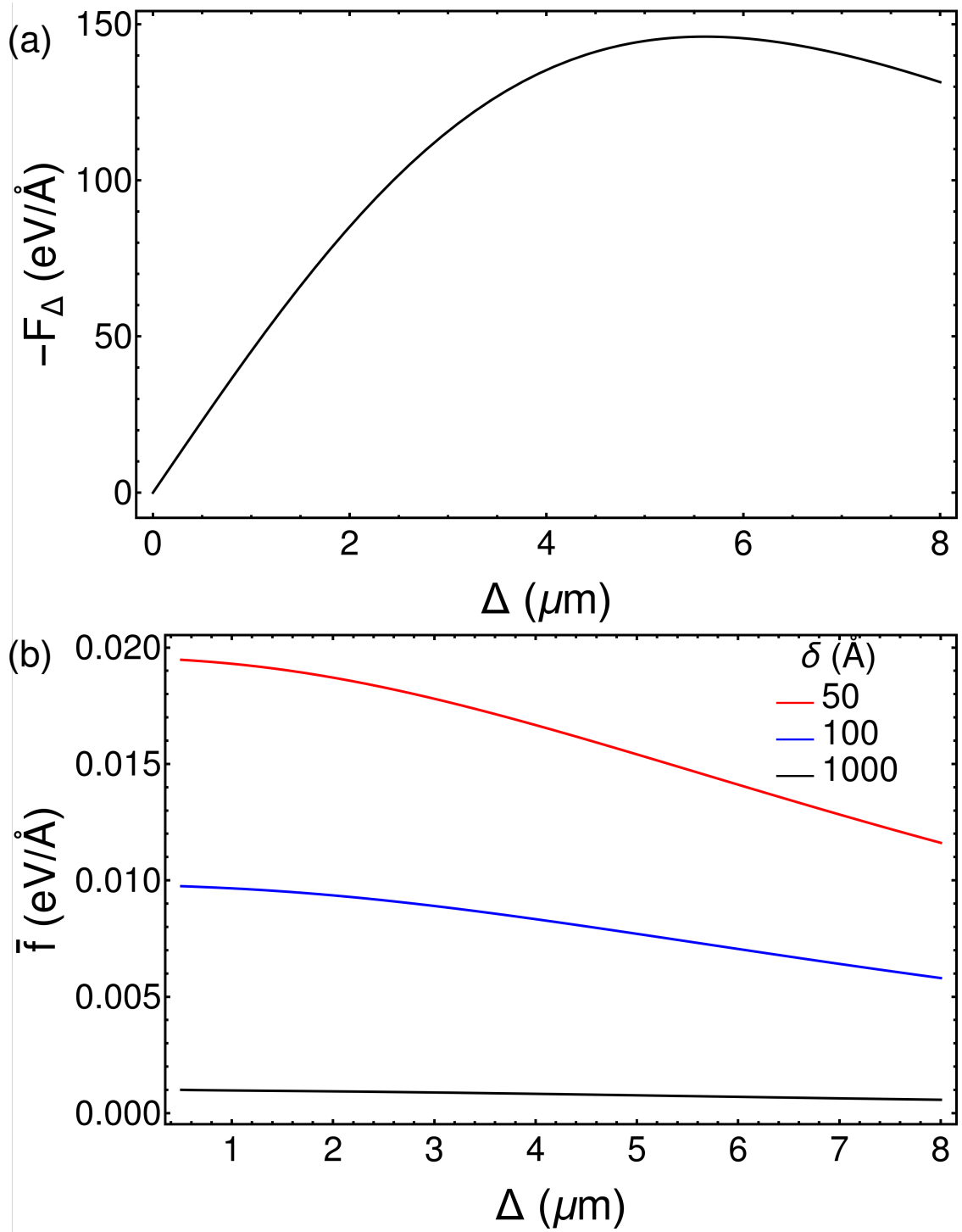
FIG. 2. (a) The generalized force on the decoupling boundary plotted as a function of Δ. (b) An estimate of the average force per atom experienced by atoms with $\Delta - \delta \leq r \leq \Delta$ computed as described in the text plotted vs. Δ for three different values of δ. The magnitudes of these forces are approximately two orders of magnitude below the range associated with covalent bonding.

With the droplet present, the total energy of the system is given by

$$E = 2\pi \left(\varepsilon_o \Delta\right)^2 \left(\lambda + \mu\right) + \pi \Delta^2 \gamma_{sl} +$$
$$+ 2\pi \left(\int_\Delta^{r_0} \left(\gamma_{sl} + E_s\right) r \, dr + \int_{r_0}^R \left(\gamma_{sv} + E_s\right) r \, dr\right) +$$
$$+ \gamma_{lv} A_{lv}, \tag{9}$$

where the first two terms on the right hand side correspond to the elastic and interfacial energy in the $0 \leq r < \Delta$ region, respectively; A_{lv} is the liquid-vapor interface area; and E_s is the strain energy density, that can be written as[28]

$$E_s[u(r), u'(r)] = \frac{\left(\lambda + 2\mu\right)\left(r^2 u'(r)^2 + u(r)^2\right) + 2\lambda r u(r) u'(r)}{2r^2}. \tag{10}$$

An underlying assumption in Eqn. (9) is that, as the number of film atoms in contact with the liquid or the vapor phase is a function only of r_0, the film deformation state for the calculation of the solid-liquid and -vapor interfacial energies is neglected.

As A_{lv} can be written as a function of u_0 and r_0 (see Appendix B), Eqn. (9) is a functional of the in-plane displacement $u(r)$, and depends too on r_0. Thus, the tools of variational calculus are suitable to study this system (for an introduction to the topic, see, *e.g.*, Ref.[29]).

The in-plane displacement function can be defined as a piecewise function

$$u(r) = \begin{cases} r\varepsilon_o & r < \Delta \\ u_1(r) & \Delta \leq r \leq r_0 \\ u_2(r) & r_0 \leq r \leq R, \end{cases} \tag{11}$$

subject to boundary conditions

$$u_1(r_0) = u_2(r_0) = u_0 \text{ and}$$
$$u_1(\Delta) = \varepsilon_o \Delta. \tag{12}$$

Computing the variation of the total energy, δE by varying functions u_1 and u_2, along with the r_0 parameter, one obtains:

$$\delta E = \tag{13}$$

$$\int_\Delta^{r_0} \left(F_{1,u_1} - \frac{d}{dr} F_{1,u_1'}\right) \delta u_1 dr \tag{13a}$$

$$+ \int_{r_0}^R \left(F_{2,u_2} - \frac{d}{dr} F_{2,u_2'}\right) \delta u_2 dr \tag{13b}$$

$$+ \left(F_1 - u_1' F_{1,u_1'} - F_2 + u_2' F_{2,u_2'} + \gamma_{lv} A_{lv,r_0}\right)\Big|_{r=r_0} \delta r_0 \tag{13c}$$

$$+ \left(F_{1,u_1'} - F_{2,u_2'} + \gamma_{lv} A_{lv,u_0}\right)\Big|_{r=r_0} \delta u_0 \tag{13d}$$

$$+ \left(F_{2,u_2'}\right)\Big|_{r=R} \delta u_2(R), \tag{13e}$$

where

$$F_i = 2\pi r \left(\gamma_{si} + E_s[u_i(r), u_i'(r)]\right), \tag{14}$$

$\gamma_{s1} = \gamma_{sl}$, $\gamma_{s2} = \gamma_{sv}$, and a subscript after a comma denotes differentiation with respect to the quantity following the comma. Since all the variations are arbitrary, one can assume that each of the terms (13a) - (13e) of Eqn. (13) vanish independently.

Consider terms (13a) and (13b) of Eqn. (13). Since δu_i is an arbitrary variation, one concludes that $F_{i,u} - \frac{d}{dr} F_{i,u'} = 0$. Using the definition of F_i, Eqn. (14), and solving the resulting second order differential equation, one finds

$$u_i(r) = a_{i1} r + \frac{a_{i2}}{r}, \tag{15}$$

where a_{ij} are constants to be determined. Using the boundary conditions (12), and setting term (13e) equal to zero, it is possible to write three of the undetermined constants a_{ij} in terms of a_{11}:

$$a_{12} = \Delta^2(\varepsilon - a_{11}),$$
$$a_{21} = \mu \frac{a_{11}\left(r_0^2 - \Delta^2\right) + \Delta^2\varepsilon}{r_0^2\mu + R^2(\lambda + \mu)},$$
$$a_{22} = R^2(\lambda + \mu)\frac{a_{11}\left(r_0^2 - \Delta^2\right) + \Delta^2\varepsilon}{r_0^2\mu + R^2(\lambda + \mu)}. \tag{16}$$

An analytical expression for a_{11} as a function of r_0 can be derived from setting term (13d) to zero. Lastly, it is possible to compute a numerical value for r_0 by setting term (13c) to zero. Then, with this solution, the equilibrium configuration of the system and its energy are determined from Eqns. (9), (15), and (16), along with the expression for a_{11} and the numerical value of r_0.

III.   RESULTS AND DISCUSSION

The hypothesis investigated here assumes that the strained film will be near instability, and that the strain release will be governed by a type of near-critical behavior found in other systems governed by stick/slip friction. Theoretical analysis of pinned charge density waves[30], earthquake fault slipping[31] and dislocation motion[32–34] all show that in such systems, a small perturbation force can lead to a large scale response. In the present case, we propose that a small perturbative force can initiate the slipping process that relaxes the film.

In this framework, then, all that is needed is for the droplet to provide the necessary perturbing force. The theory presented here shows that there is an in-plane force arising from the liquid/vapor/solid intersection.

If the droplet is considered, the elastic state of the film is a function of the interfacial energies γ_{ij}, meaning that it will be different from that shown in Sec. II A. To understand the extra force provided by this perturbation, we begin by comparing the in-plane displacements u of the equilibrium configuration in systems with and without a droplet, Fig. 3. For the chosen interfacial tensions [which correspond to $\theta < \pi/2$ in Eqn. (8)], the displacements within the decoupled region are reduced relative to the values that they have in the absence of the droplet. *The implication is that the droplet places the region $\Delta < r < r_0$ under compression relative to the droplet-free case.* This additional compressive strain exerts a force on the boundary of the decoupled region tending to decrease Δ. Hence, for the chosen parameters, the presence of a droplet with $\Delta < r_0 < R$ increases the decoupling force.

Note that the increase in decoupling force is of the order of a few percent (see Fig. 4) – an amount consistent with the notion that the films are near instability. That the extra force increases with the droplet volume may explain why sometimes, as reported in Ref.[7], it takes several droplet applications in order to fully relax the film. As the the volume of the droplet decreases due to evaporation, the extra force may fall below the threshold necessary to trigger decoupling causing the radius of the contact patch of the droplet to fall below Δ. Reapplying another, larger drop, increases the force, and enables decoupling to proceed.

Also note that in the presence of the strain, the contact angle defined by Eqn. (8) is not the final contact angle of the fluid. Since the film is strained, and the strain exerts a force on the triple point, the contact angle is altered slightly. The angle might be decreased or increased depending upon the sign of the stress, and the value of the contact angle for an unstressed film.

In addition, the circular shape of the film assumed in our model is different than that of the experiments described in Ref.[7] (triangular). The circular geometry was chosen as it leads to an axisymmetric model that can be solved relatively easily. While the geometry of the film may alter the shape of the contact patch for the droplet and the film, the underlying physical processes will remain very similar, and the insights from the circular model will be helpful in understanding the release of the triangular samples.

The change from a circular geometry to a triangular one also results in more atoms at the edge of the film, and it is reasonable to expect that these atoms might be bonded more strongly to the substrate than atoms in the interior of the film. The model does not account for differences between interior and edge atoms, but experimental results[7] prove that the force exerted by the droplet is enough to overcome any force due to extra bonds that the edge atoms might have with the substrate.

A.   Conditions Under Which Evaporation of a Droplet Will Release Strain

In order to assess the conditions in which the SEMD is possible, one has to consider how the system will behave for a variety of parameter sets and strains. Though the mathematics underlying the effect of an evaporating droplet
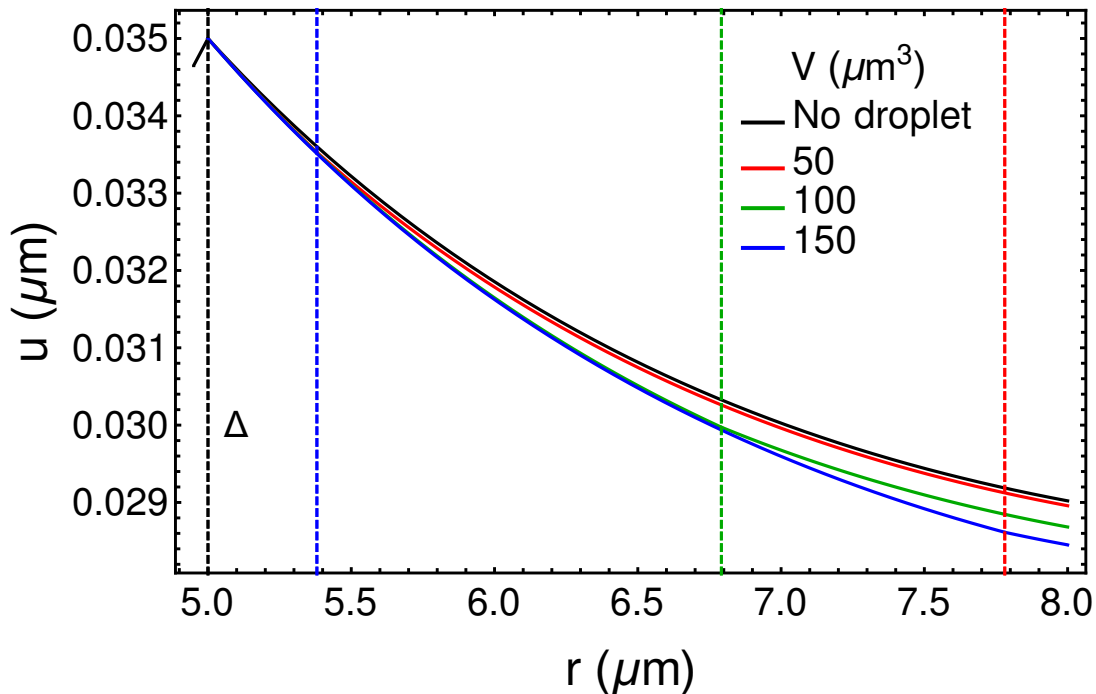
FIG. 3. In-plane displacement in the equilibrium configuration for a system with $\Delta = 5\,\mu m$ and different liquid volumes. The vertical black line corresponds to $r = \Delta$, while the others correspond to $r = r_0$ for the different values of V

are subtle, there is a simple way to qualitatively predict the effects of droplet evaporation on the decoupling. If the in-plane projection of the liquid-vapor interfacial tension anti-aligns with the radial displacements arising from the initial strain (radially outwards if $\varepsilon_o > 0$, radially inwards if $\varepsilon_o < 0$), the evaporation will increase the net force on the decoupling interface, and can lead to decoupling. Conversely, if the projection of the liquid-vapor interfacial tension is aligned with the displacements associated with ε_0, the evaporating droplet will tend to stabilize the strain state. The applicability of this simple assessment is presented in Fig. 5. This figure shows, for a variety of contact angles as defined by Eqn. (8), the displacements, $u_d(r)$ and the strains $\varepsilon_d(r) = u_d'(r)$, induced by the application of an evaporating droplet. Note that the displacements plotted here are computed according to

$$u_d(r) = u^{\text{with droplet}}(r) - u^{\text{without droplet}}(r) \tag{17}$$

with $u^{\text{with droplet}}(r)$ and $u^{\text{without droplet}}(r)$ referring to the solutions for the displacements with and without the droplet, respectively. From the ε_d plots shown in the third column of Fig. 5, one can see the effect the droplet has on the decoupling force F_Δ: if ε_d is of the opposite sign of ε_o in the $\Delta < r < r_0$ region, as in cases I and IV, then the decrease in the elastic energy prompted by a decrease in Δ is bigger than in the no droplet case, thus increasing $|F_\Delta|$, and the droplet has the potential to initiate strain release. In contrast, in cases II and III, the strain release will not be initiated.

IV. CONCLUSIONS

A theoretical model for the SEMD method for as-grown strain release in a film is developed and analyzed. The model demonstrates that bond strengths well below those of covalent bonds are likely sufficient to stabilize the strains arising during the van der Waals epitaxial growth of the WSe$_2$. The model also predicts that a droplet of liquid can generate an additional in-plane force that can trigger the decoupling of the film from the substrate. Specifically, if the contact angle of the liquid is such that the projection of the liquid/vapor surface tension is anti-aligned with the elastic displacements of the coupled film, then the in-plane force has the potential to trigger decoupling.

The origin of the extra decoupling force is the compression (or tension, depending upon the system in question) of the outer portion of the film that is free to slide. This additional strain arises from the interfacial tensions associated with the droplet/film/vapor triple point. For the acetone/WSe$_2$ strained in tension samples, the extra compression of the free sliding region from the droplet can be relieved if more of the film decouples by reducing Δ, and the droplet
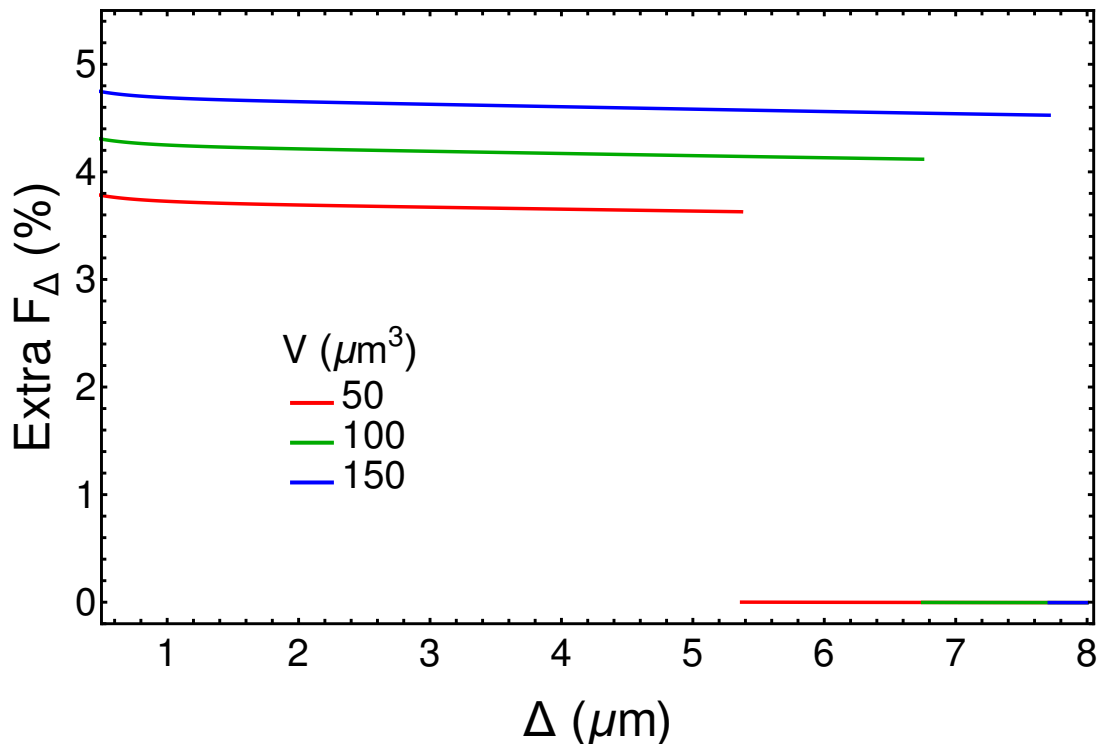
FIG. 4. Percentage increase in decoupling force (now elastic plus droplet effects) relative to just the elastic force for three different droplet volumes plotted as a function of Δ. The step discontinuity at larger Δ arises from the fact that, within the model, there is no extra force if the radius of the pinned region is larger than the radius of the droplet contact patch.

can initiate strain release. The extra decoupling force represents an approximate 4% increase in the decoupling force for the specific case of an acetone droplet and a WSe$_2$ film grown on amorphous silica.

Based on the model, it may be possible to use the SEMD method with a wide range of substrates and 2D materials beyond TMDCs, opening the possibility of creating complex relaxation patterns that exploit the strain tuned direct-to-indirect bandgap change[3] to create novel devices. The fundamental understanding of the origins of the extra force provided by the droplet, and the predictions outlined in Fig. 5, make the case for the SEMD method to be a viable pathway to engineer strain in 2D materials, thereby harnessing the variety of strain-tunable properties[35].

V.   ACKNOWLEDGEMENTS

Appendix A: Out-of-plane displacement

Allowing for the film to have out-of-plane (OOP) displacements will change the model in three main ways. First, some of the liquid will be wrapped by the film, resulting in a decrease of A_{lv}; if this is to happen spontaneously, this will necessarily decrease the liquid-vapour interfacial energy. Second, the substrate-film interaction has to be taken into account. Finally, the elastic energy of the film, previously given by (10), needs to be modified to account for the OOP displacement. We can estimate the extent of the OOP displacements by looking at how the energy of the system changes when these additional terms are considered.

The deformation map of the film is given by $\{r, 0\} \rightarrow \{r + u(r), f(r)\}$, where $f(r)$ is the OOP displacement at radius r. If the film is lifted at r_0, a portion V_w of the liquid volume V will be wrapped by the film. Assuming that the length of the OOP feature of the film near r_0 is small compared to R, and that far from r_0 the film is at the
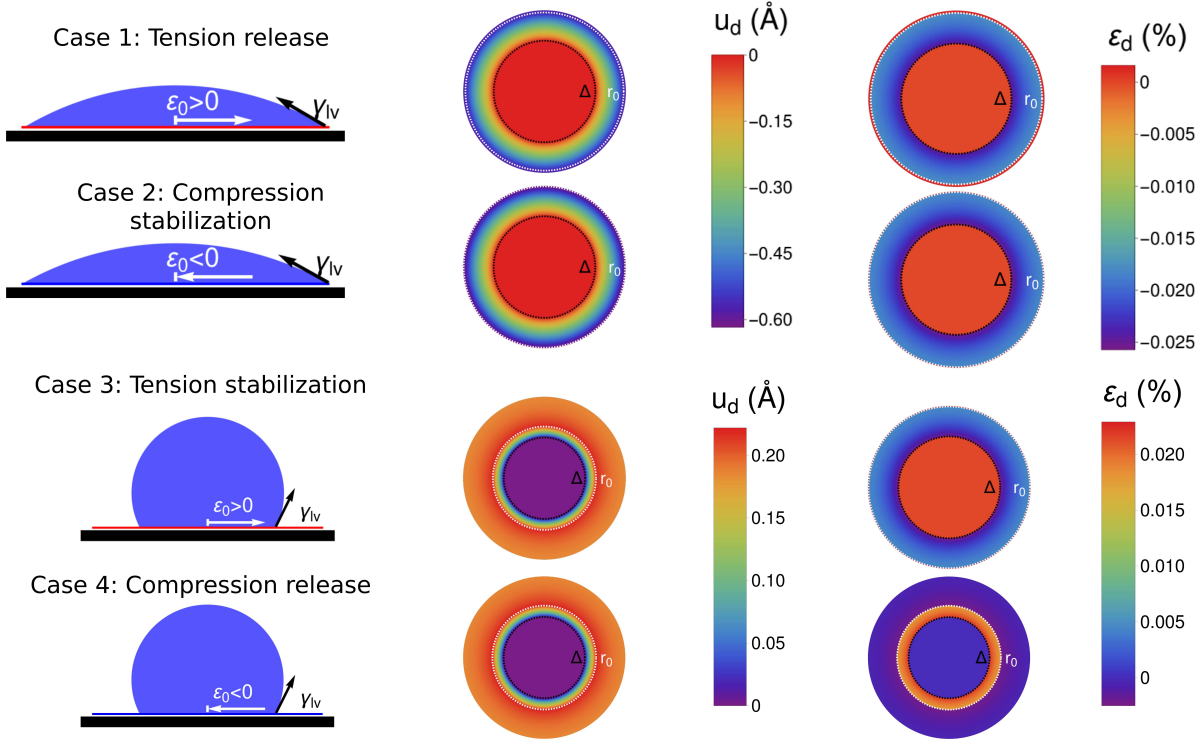
FIG. 5. Schematics, displacement and strains for a droplet on top of a strained film. For cases 3 and 4, a volume of $V = 500\,\mu m^3$ was used; $\gamma_{lv} = 0.45\,\mathrm{MeV}^2\,\mu m^{-1}$ and $\gamma_{sl} = 0.40\,\mathrm{MeV}^2\,\mu m^{-1}$ were selected so that γ_{lv} would match that of water and the Young's angle, defined by Eqn. (8), was 110°. Cases 2 and 4 use an initial strain of $\varepsilon_o = -0.7\%$. The white arrows indicate the direction of the displacements associated with the strain. For cases 1 and 4, the droplet has the potential to initiate decoupling of the film from the substrate. For cases 2 and 3, the droplet will likely stabilize the strain state.

equilibrium height (set at $f(r) = 0$), we have

$$V_w = 2\pi \int_0^{r_0} (r + u(r))) \left(1 + u'(r)\right)(f_0 - f(r))\,dr \approx \pi f_0 \left(r_0 + u_0\right)^2, \tag{A1}$$

where $f_0 = f(r_0)$. Then, the liquid-vapour interaction energy is given by

$$E_{lv} = \gamma_{lv} A_{lv} (V - V_w) \tag{A2}$$

(an expression for $A_{lv}(V)$ is given in Appendix B).

The substrate-film interaction energy is fit to a Morse potential:

$$E_{subs-film} = 2\pi \int_0^R r D_e \left\{1 - \exp\left[-\beta\left(r - r_{eq}\right)\right]\right\}^2 dr, \tag{A3}$$

where D_e, β are constants. To determine D_e and β, Density Functional Theory (DFT) computations were run using the Vienna Ab initio Simulation Package[36–38] version 5.4.4. The projected-augmented-wave method was used to model the core electrons[39], and the exchange-correlation energy was estimated using Perdew-Burke-Ernzehof potentials[40]. All the simulations were run using a $500\,\mathrm{eV}$ cutoff energy for the plane-wave basis set, a Γ-centered k-point $8 \times 8 \times 1$ grid, and convergence criteria of $10^{-4}\,\mathrm{eV}$ for the electronic self-consistent cycle. The simulations consisted in a 27 layer slab of α-SiO$_2$ with a reconstructed (001) surface, as reported in Ref.[41]; a 3×3 monolayer WSe$_2$ supercell was positioned on top of the SiO$_2$; to obtain a commensurate structure, the SiO$_2$ was put under a -0.3% biaxial compression. The parameters in Eqn. (A3) were obtained by fitting the energies obtained by DFT, the results being $D_e = 0.50\,\mathrm{meV}\,\text{Å}^{-2}$ and $\beta = 1.31\,\text{Å}^{-1}$. The energies, along with a the Morse fit, are shown in Fig. 6.

The elastic energy will now have to account for the bending energy. Using linear elasticity theory, we find:

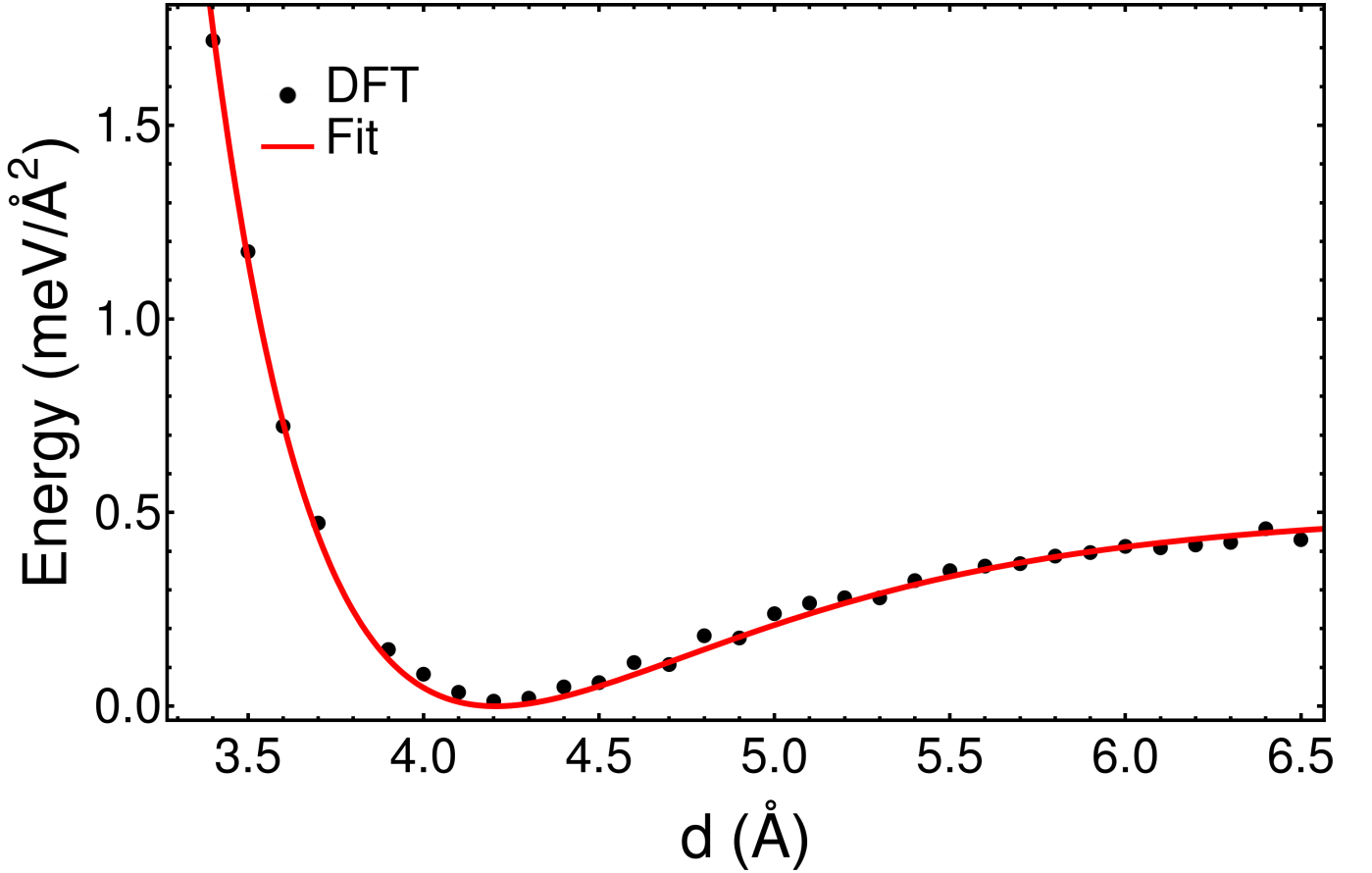$$E_{bending} = \pi\kappa \int_0^R r \left(\frac{f'(r)}{r} + f''(r)\right)^2 dr, \tag{A4}$$

FIG. 6. Energy of WSe_2/SiO_2 system as a function of the film-substrate separation, d. The solid line is Eqn. (A3) using $D_e = 0.50\,\mathrm{meV}\,\text{Å}^{-2}$ and $\beta = 1.31\,\text{Å}^{-1}$

where $\kappa = 11.25\,\mathrm{eV}^{42}$ is the bending rigidity. Also, the strain energy density is modified to incorporate OOP displacement:

$$E_s = \frac{1}{8}(\lambda + 2\mu)\left(f'(r)^2 + 2u'(r)\right)^2 + \frac{\lambda u(r)\left(f'(r)^2 + 2u'(r)\right)}{2r} + \frac{(\lambda + 2\mu)u(r)^2}{2r^2}. \tag{A5}$$

Using a Gaussian-like function for the OOP displacement,

$$f(r) = f_0 \exp\left[-\frac{(r - r_0)^2}{\sigma}\right], \tag{A6}$$

and Eqns. (A2-A5), the energy of the system was evaluated, and the differences in energy of these systems compared to the case were no OOP displacement is allowed, ΔE_{OOP}, are plotted in Fig. 7. Note that, as we are not solving the variational equations for this case, the form of the displacements used to obtain the energies shown in Fig. 7 are not the ones that minimize the energy; this is justified because the goal of this appendix is not to determine a precise value for f_0, but rather to assess its orders of magnitude. The values reported in the figure were obtained by choosing the value of σ to minimize the energy change for each value of f_0; for the reported f_0 range, it was found that the values of σ that minimized the energy were in the $240\,\text{Å}^2 < \sigma < 250\,\text{Å}^2$ range, corresponding to an OOP displacement feature of $\sim 50\,\text{Å}$. Fig. 7 shows that, even though lifting the film near results in a reduced system energy, the f_0 range in which this happen is very narrow, with the minimum happening around $f_0 = 0.0125\,\text{Å}$. This level of OOP displacements will not alter much the analysis as compared to assuming no OOP, and is consequently neglected.
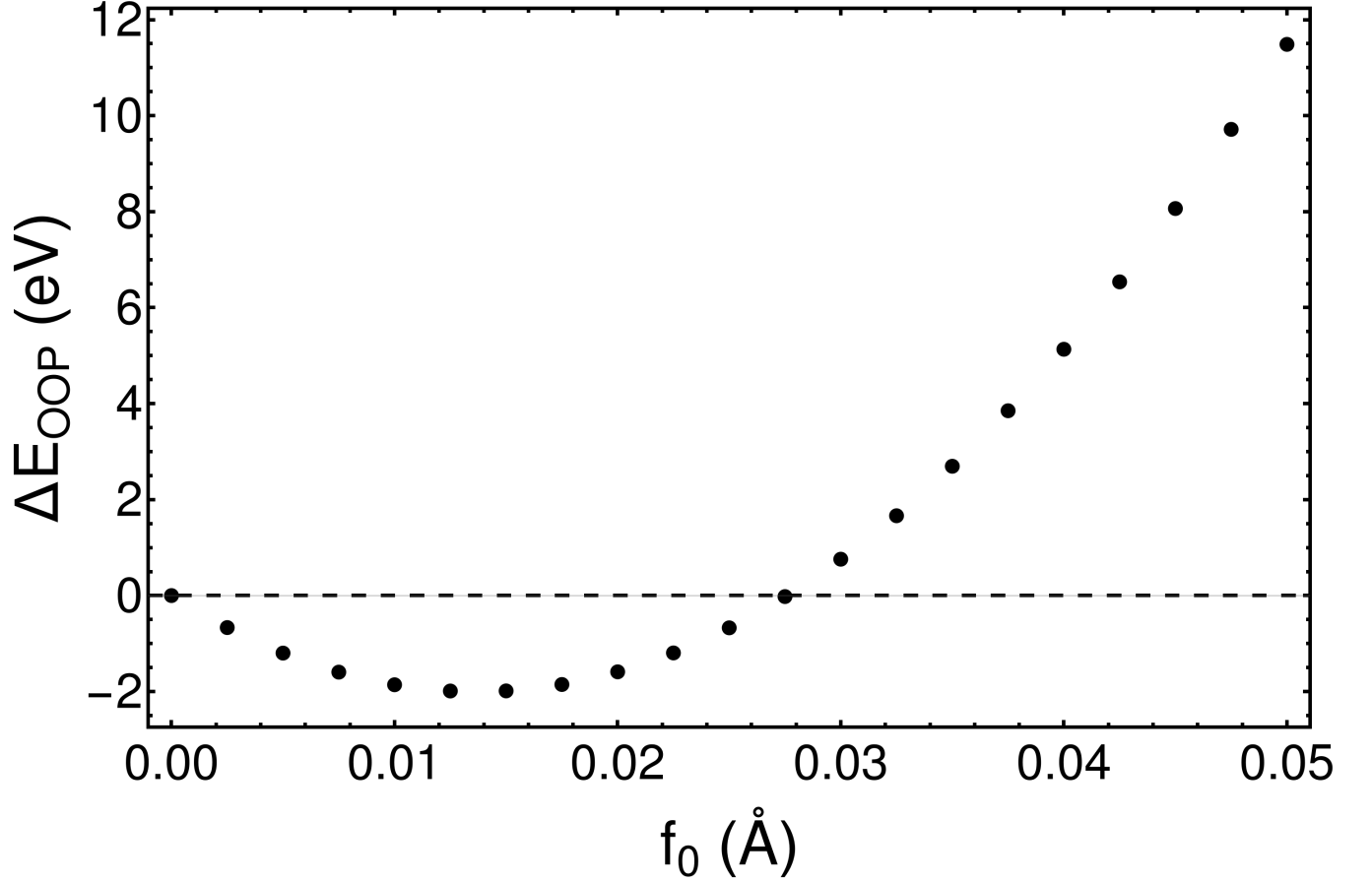
FIG. 7. Energy differences of systems with and without OOP displacement. The parameters used where those shown in Table I, $V = 150\,\mu m^3$, $\Delta = 5\,\mu m$. The values for r_0 and u_0 were obtained using the formalism shown in Sec. II B.

Appendix B: Liquid-vapor interface area (A_{lv}) expression

The volume of a spherical cap with base radius $d = r_0(1 + \varepsilon)$ and contact angle θ is given by

$$V = \frac{\sqrt{A_{lv}}\left(A_{lv} + 2\pi d^2\right)\sqrt{1 - \frac{\pi d^2}{A_{lv}}}}{6\sqrt{\pi}}. \tag{B1}$$

Solving for A_{lv}, linearizing in the strain ε, and then doing the replacement $\varepsilon r_0 \to u_0$, one finds:

$$
\begin{aligned}
A_{lv}(V) = & \frac{2\pi^{7/3} r_0^5 u_0 \left(\sqrt{\pi^2 r_0^6 + 9V^2} + 3V\right)}{\sqrt{\pi^2 r_0^6 + 9V^2}\left(6V\left(\sqrt{\pi^2 r_0^6 + 9V^2} + 3V\right) + \pi^2 r_0^6\right)^{2/3}} + \\
& + \frac{\pi^{5/3} r_0^3 \left(2u_0\left(\sqrt{\pi^2 r_0^6 + 9V^2} + 3V\right) + r_0\sqrt{\pi^2 r_0^6 + 9V^2}\right)}{\sqrt{\pi^2 r_0^6 + 9V^2}\left(6V\left(\sqrt{\pi^2 r_0^6 + 9V^2} + 3V\right) + \pi^2 r_0^6\right)^{1/3}} + \\
& + \left(6\pi V\left(\sqrt{\pi^2 r_0^6 + 9V^2} + 3V\right) + \pi^3 r_0^6\right)^{1/3} - \pi r_0(r_0 + 2u_0).
\end{aligned}
\tag{B2}
$$

Appendix C: Full derivation of equations

1. Variational equation: Eqn. (13)

We start by deriving the energy variational, Eqn. (13). To do this, it is useful to group the full energy of the system, Eqn. (9), as follows:

$$E = \underbrace{\int_\Delta^{r_0} F_1[u_1(r), u_1'(r), r]\, dr}_{E_1} + \underbrace{\int_{r_0}^R F_2[u_2(r), u_2'(r), r]\, dr}_{E_2} + \phi(r_0, u_0), \tag{C1}$$

where

$$\phi(r_0, u_0) = 2\pi\, (\varepsilon_o \Delta)^2\, (\lambda + \mu) + \pi \Delta^2 \gamma_{sl} + \gamma_{lv} A_{lv}(r_0, u_0). \tag{C2}$$

Then, the variational of the energy can be written as

$$\delta E = \delta E_1[u_1, u_1'; r_0] + \delta E_2[u_2, u_2'; r_0] + \delta\phi(r_0, u_0), \tag{C3}$$

where E_1 and E_2 are functionals of the in-plane displacement u, u', and also depend on r_0; on the other hand, ϕ is a function of the parameters r_0 and u_0. As there are no physical constraints for the values of $u_1(r_0)$, $u_2(r_0)$, and $u_2(R)$ (that is, other than the continuity constraint $u_1(r_0) = u_2(r_0)$) natural boundary conditions (NBCs) are used. Thus, the variationals of the individual terms in Eqn. (C3) are given by

$$\delta E_1 = \int_\Delta^{r_0} \left(F_{1,u_1} - \frac{d}{dr} F_{1,u_1'} \right) \delta u_1 dr +$$

$$+ \left(F_1 - u_1' F_{1,u_1'} \right)\bigg|_{r=r_0} \delta r_0 +$$

$$+ F_{1,u_1'}\bigg|_{r=r_0} \delta u_1(r_0), \tag{C4}$$

$$\delta E_2 = \int_\Delta^{r_0} \left(F_{2,u_2} - \frac{d}{dr} F_{2,u_2'} \delta u_2 dr \right) +$$

$$+ F_{2,u_2'}\bigg|_{r=R} \delta u_2(R) +$$

$$- \left(F_2 - u_2' F_{2,u_2'} \right)\bigg|_{r=r_0} \delta r_0 +$$

$$- F_{2,u_2'}\bigg|_{r=r_0} \delta u_2(r_0), \tag{C5}$$

$$\delta\phi = \phi_{,r_0} \delta r_0 + \phi_{,u_0} \delta u_0, \tag{C6}$$

where the functional dependencies have been obviated. Finally, as $u_1(r_0) = u_2(r_0) = u_0$, we arrive at Eqn. (13) simply by grouping terms.

We can arrive to Eqn. (15) by considering that, for an extremum point, $\delta E = 0$; then, as δu_i is arbitrary, the integrand in Eqns. (13a) and (13b) should be zero. Using the definition of F_i, Eqn. (14), we then find that

$$F_{i,u_i} - \frac{d}{dr} F_{i,u_i'} = 0 \Rightarrow$$

$$\frac{(\lambda + 2\mu)\, u_i + r\lambda u_i'}{r} - [2(\lambda + \mu)\, u_i' + r(\lambda + 2\mu)\, u_i''] = 0 \Rightarrow$$

$$u_i - ru_i' - r^2 u_i'' = 0 \Rightarrow$$

$$u_i = a_{i1}r + \frac{a_{i2}}{r}. \tag{C7}$$

Now we obtain expressions for the constants a_{ij}. Analyzing the NBC set in Eqn. (13d), we get

$$F_{2,u_2'}|_{r=R} = 0 \Rightarrow$$

$$\frac{a_{22}\mu}{R} = a_{21}R(\lambda + \mu). \tag{C8}$$

Solving for a_{12}, a_{21}, a_{22} in the boundary conditions Eqns. (12) and (C8) we get Eqns. (16). It is possible to get an analytical expression for a_{11} by using the NBC set by Eqn. (13d) and plugging in the expressions of the other constants; however, the expression is very long and not very enlightening.

2. Energy and displacement in a strained disc: Eqns. (1) and (2)

While there are many ways to obtain the energy and the displacement of a strained disc, here, to maintain the spirit of the paper, we will opt for an energy minimization using a variational approach.

The energy of the system without a droplet is given by

$$E_{nd} = 2\pi\Delta^2(\lambda+\mu)\varepsilon_o^2 + 2\pi\int_\Delta^R E_s r dr, \tag{C9}$$

i.e., the energy of the system is only due to its strain state. The variational of Eqn. (C9) is then

$$\delta E_{nd} = \tag{C10}$$

$$\int_\Delta^R \left(G_{,u} - \frac{d}{dr}G_{,u'}\right)\delta u dr+ \tag{C10a}$$

$$+ \left.(G_{,u'})\right|_{r=R} \delta u(R), \tag{C10b}$$

where $G = G[u(r), u'(r)] = 2\pi r E_s[u(r), u'(r)]$, and we have assumed NBCs at $u(R)$. As δu in Eqn. (C10a) is arbitrary, the integrand should be set to zero. Then, for an extremum point, we have that

$$G_{,u} - \frac{d}{dr}G_{,u'} = 0 \Rightarrow$$

$$\frac{(\lambda+2\mu)u + r\lambda u'}{r} - [2(\lambda+\mu)u' + r(\lambda+2\mu)u''] = 0 \Rightarrow$$

$$u - ru' - r^2 u'' = 0 \Rightarrow$$

$$u = a_1 r + \frac{a_2}{r}, \tag{C11}$$

where a_i are constants to be determined from the boundary conditions. One boundary condition comes from the in-plane-displacement continuity, $u(\Delta) = \varepsilon_o\Delta$, while the other comes from Eqn. (C10b). Solving for the a_i constants, we get

$$a_1 = \frac{\Delta^2\varepsilon_o\mu}{\Delta^2\mu + R^2(\lambda+\mu)},$$

$$a_2 = \frac{R^2\Delta^2\varepsilon_o(\lambda+\mu)}{\Delta^2\mu + R^2(\lambda+\mu)}. \tag{C12}$$

Finally, inserting Eqn. (C12) into (C11), we get Eqn. (2), and inserting this expression for the in-plane-displacement into the energy of the system, Eqn. (C9), gives us Eqn. (1).

[*] dcchrzan@berkeley.edu
[1] Sheneve Z. Butler, Shawna M. Hollen, Linyou Cao, Yi Cui, Jay A. Gupta, Humberto R. Gutiérrez, Tony F. Heinz, Seung Sae Hong, Jiaxing Huang, Ariel F. Ismach, Ezekiel Johnston-Halperin, Masaru Kuno, Vladimir V. Plashnitsa, Richard D. Robinson, Rodney S. Ruoff, Sayeef Salahuddin, Jie Shan, Li Shi, Michael G. Spencer, Mauricio Terrones, Wolfgang Windl, and Joshua E. Goldberger. Progress, challenges, and opportunities in two-dimensional materials beyond graphene. *ACS Nano*, 7(4):2898–2926, 2013.
[2] Qing Hua Wang, Kourosh Kalantar-Zadeh, Andras Kis, Jonathan N. Coleman, and Michael S. Strano. Electronics and optoelectronics of two-dimensional transition metal dichalcogenides. *Nat. Nanotechnol.*, 7(11):699–712, 2012.
[3] Rafael Roldán, Andrés Castellanos-Gomez, Emmanuele Cappelluti, and Francisco Guinea. Strain engineering in semiconducting two-dimensional crystals. *J. Phys.: Condens. Matter*, 27(31), 2015.

[4] Hiram J. Conley, Bin Wang, Jed I. Ziegler, Richard F. Haglund, Sokrates T. Pantelides, and Kirill I. Bolotin. Bandgap engineering of strained monolayer and bilayer MoS2. *Nano Lett.*, 13(8):3626–3630, 2013.

[5] Yeung Yu Hui, Xiaofei Liu, Wenjing Jie, Ngai Yui Chan, Jianhua Hao, Yu Te Hsu, Lain Jong Li, Wanlin Guo, and Shu Ping Lau. Exceptional tunability of band energy in a compressively strained trilayer MoS2 sheet. *ACS Nano*, 7(8):7126–7131, 2013.

[6] Geun Ho Ahn, Matin Amani, Haider Rasool, Der Hsien Lien, James P. Mastandrea, Joel W. Ager, Madan Dubey, Daryl C. Chrzan, Andrew M. Minor, and Ali Javey. Strain-engineered growth of two-dimensional materials. *Nat. Commun.*, 8(1):1–7, 2017.

[7] Hyungjin Kim, Geun Ho Ahn, Joy Cho, Matin Amani, James P Mastandrea, Catherine K Groschner, Der-hsien Lien, Yingbo Zhao, Joel W. Ager, Mary C Scott, Daryl C Chrzan, and Ali Javey. Synthetic WSe 2 monolayers with high photoluminescence quantum yield. *Sci. Adv.*, 5(1):eaau4728, 2019.

[8] Teodor M Atanackovic and Ardéshir Guran. *Theory of elasticity for scientists and engineers.* Springer Science & Business Media, 2000.

[9] Michel Grandbois, Martin Beyer, Matthias Rief, Hauke Clausen-Schaumann, and Hermann E. Gaub. How strong is a covalent bond? *Science*, 283(5408):1727–1730, 1999.

[10] Ji Guo, H. Batiz, and D. C. Chrzan. Unpublished research. 2021.

[11] In appendix A it is argued that the effects of lifting of the film by the liquid-vapor surface tension are negligible with respect to the estimate of the magnitude of the forces involved. Nevertheless, the expected width of the lifted region is of the order of 50 Å. The width of this lifted region sets a natural scale for δ when the liquid is present.

[12] Deniz ÇakIr, François M. Peeters, and Cem Sevik. Mechanical and thermal properties of h -MX2(M = Cr, Mo, W; X = O, S, Se, Te) monolayers: A comparative study. *Appl. Phys. Lett.*, 104(20), 2014.

[13] Meenakshi Annamalai, Kalon Gopinadhan, Sang A. Han, Surajit Saha, Hye Jeong Park, Eun Bi Cho, Brijesh Kumar, Abhijeet Patra, Sang Woo Kim, and T. Venkatesan. Surface energy and wettability of van der Waals structures. *Nanoscale*, 8(10):5764–5770, 2016.

[14] Joseph J. Jasper. The Surface Tension of Pure Liquid Compounds. *J. Phys. Chem. Ref. Data*, 1(4):841–1010, 1972.

[15] Victor M Starov, Manuel G Velarde, and Clayton J. Radke. *Wetting and Spreading dynamics.* 2007.

[16] R. Kern and P. Müller. Deformation of an elastic thin solid induced by a liquid droplet. *Surf. Sci.*, 264(3):467–494, 1992.

[17] Lee R. White. The contact angle on an elastic substrate. 1. The role of disjoining pressure in the surface mechanics. *J. Colloid Interface Sci.*, 258(1):82–96, 2003.

[18] Elizabeth R. Jerison, Ye Xu, Larry A. Wilen, and Eric R. Dufresne. Deformation of an elastic substrate by a three-phase contact line. *Phy. Rev. Lett.*, 106(18):1–4, 2011.

[19] Ying Song Yu. Circular plate deformed by a sessile droplet. *J. Adhes. Sci. Technol.*, 28(19):1970–1979, 2014.

[20] Soon Hong Yuk and Mu Shik Jhon. Contact angles on deformable solids. *J. Colloid Interface Sci.*, 110(1):252–257, 1986.

[21] Didier Long, Armand Ajdari, and Ludwik Leibler. Static and dynamic wetting properties of thin rubber films. *Langmuir*, 12(21):5221–5230, 1996.

[22] Ying Song Yu. Substrate elastic deformation due to vertical component of liquid-vapor interfacial tension. *Appl. Math. Mech.-Engl.*, 33(9):1095–1114, 2012.

[23] Heyi Liang, Zhen Cao, Zilu Wang, and Andrey V. Dobrynin. Surface Stresses and a Force Balance at a Contact Line. *Langmuir*, 34(25):7497–7502, 2018.

[24] Zhen Cao and Andrey V. Dobrynin. Polymeric droplets on soft surfaces: From Neumann's triangle to Young's law. *Macromolecules*, 48(2):443–451, 2015.

[25] Martin E.R. Shanahan. Contact Angle Equilibrium on Thin Elastic Solids. *J. Adhes.*, 18(4):247–267, 1985.

[26] M. E.R. Shanahan. The influence of solid micro-deformation on contact angle equilibrium. *J. Phys. D*, 20(7):945–950, 1987.

[27] Martin E.R. Shanahan. Equilibrium of liquid drops on thin plates; plate rigidity and stability considerations. *J. Adhes.*, 20(4):261–274, 1987.

[28] H. S. Seung and David R. Nelson. Defects in flexible membranes with crystalline order. *Phys. Rev. A*, 38(2):1005–1018, 1988.

[29] Vladimir Ivanovich Smirnov. *A Course of Higher Mathematics: Vol. 4, Integral Equations and Partial Differential Equations.* Pergamon Press, 1964.

[30] Daniel S Fisher. Sliding charge-density waves as a dynamic critical phenomenon. *Phys. Rev. B*, 31(3):1396, 1985.

[31] Jean M Carlson, James S Langer, and Bruce E Shaw. Dynamics of earthquake faults. *Rev. Mod. Phys.*, 66(2):657, 1994.

[32] D. C. Chrzan and MJ Mills. Criticality in the plastic deformation of ni3al. *Phys. Rev. Lett.*, 69(19):2795, 1992.

[33] D. C. Chrzan and M. J. Mills. Criticality in the plastic deformation of $L 1_2$ intermetallic compounds. *Phys. Rev. B*, 50(1):30, 1994.

[34] D. C. Chrzan and Murray S Daw. Pinning-depinning transition in dislocation dynamics. *Phys. Rev. B*, 55(2):798, 1997.

[35] Zhiwei Peng, Xiaolin Chen, Yulong Fan, David J. Srolovitz, and Dangyuan Lei. Strain engineering of 2D semiconductors and graphene: from strain fields to band-structure tuning and photonic applications. *Light Sci. Appl.*, 9(1), 2020.

[36] G. Kresse and J. Hafner. Ab initio molecular dynamics for liquid metals. *Phys. Rev. B*, 47(1):558–561, 1993.

[37] G. Kresse and J. Furthmüller. Efficient iterative schemes for ab initio total-energy calculations using a plane-wave basis set. *Phys. Rev. B*, 54(16):11169–11186, 1996.

[38] G. Kresse and J. Furthmüller. Efficiency of ab-initio total energy calculations for metals and semiconductors using a plane-wave basis set. *Comp. Mater. Sci.*, 6(1):15–50, 1996.

[39] P. E. Blöchl. Projector augmented-wave method. *Phys. Rev. B*, 50(24):17953–17979, 1994.

[40] John P. Perdew, Kieron Burke, and Matthias Ernzerhof. Generalized gradient approximation made simple. *Phys. Rev. Lett.*,

77(18):3865–3868, 1996.

[41] Oleksandr I. Malyi, Vadym V. Kulish, and Clas Persson. In search of new reconstructions of (001) α-quartz surface: A first principles study. *RSC Adv.*, 4(98):55599–55603, 2014.

[42] Kang Lai, Wei Bing Zhang, Fa Zhou, Fan Zeng, and Bi Yu Tang. Bending rigidity of transition metal dichalcogenide monolayers from first-principles. *J. Phys. D*, 49(18), 2016.